Comparison of Surface Mouted Permanent Magnet Coaxial Radial Flux Magnetic Gears Independently Optimized for Volume, Cost, and Mass

Matthew C. Gardner
IEEE Student Member
gardner1100@tamu.edu

Benjamin E. Jack
IEEE Student Member
aggieland18@tamu.edu

Matthew Johnson
IEEE Member
mjohnson11@tamu.edu

Hamid A. Toliyat
IEEE Fellow
toliyat@tamu.edu

Advanced Electric Machines & Power Electronics Lab
Department of Electrical and Computer Engineering
Texas A&M University
College Station, TX 77843

***Abstract*—This study employs a genetic algorithm (GA) to optimize surface mounted permanent magnet coaxial radial flux magnetic gear designs using both 2D Finite Element Analysis (FEA) and 3D FEA. Specifically, the GA optimizes different designs, which are all rated for a stall torque of 500 N·m and a gear ratio of approximately 5, to independently maximize volumetric torque density (VTD), torque per dollar (TPD), and gravimetric torque density (GTD). Maximum VTDs of 274 kN·m/m^3 and 210 kN·m/m^3 were obtained with 2D and 3D simulations, respectively. Including the space required to provide an axial buffer for leakage flux resulted in a maximum leakage adjusted VTD of 162 kN·m/m^3. Maximum TPDs of 5.86 N·m/$ and 5.47 N·m/$ were obtained with 2D and 3D simulations, respectively. Maximum GTDs of 102.8 N·m/kg and 86.8 N·m/kg were obtained with 2D and 3D simulations, respectively. The results demonstrate that independently maximizing these three metrics leads to markedly different designs with widely varying performance characteristics. The most significant differences occur between the maximum VTD and maximum TPD designs, and the analysis includes a thorough discussion of the dominant design parameters driving this phenomenon. Finally, the impacts of end-effects on the optimal design parameters are also illustrated to demonstrate that consideration of these 3D effects leads to significantly different performance predictions and to different optimal design selections.**

Keywords—Direct drive, finite element analysis, genetic algorithms, magnetic gear, optimization, permanent magnet, torque density

I. Introduction

Like mechanical gears, magnetic gears transfer power between high-torque, low-speed rotation and low-torque, high-speed rotation. However, magnetic gears use the modulated interaction of magnetic fields, instead of physical contact between interlocking teeth. Therefore, magnetic gears offer a plethora of potential advantages over mechanical gears, such as inherent overload protection, improved reliability, reduced maintenance, and physical isolation between shafts. These potential advantages have resulted in significant recent interest in magnetic gears [1]-[3]. Magnetically geared systems can combine the reliability benefits of gearless, direct-drive machines with the system size and cost reduction benefits of mechanically geared systems. These advantages are especially enticing for high-torque, low-speed applications, such as wind turbines [4], wave energy generation [5], ship propulsion [6], and electric vehicles [7].

While most magnetic gear literature focuses on maximizing magnetic gears' volumetric torque densities (VTDs) to make their sizes competitive with those of mechanical gears [8], [9], improvements in other areas, such as material cost, mass, and efficiency, are also critical for this technology to achieve commercial success. However, the importance of each objective varies significantly between applications, and the optimal design parameters depend on the relative weight of each objective [10]. This study compares the designs of magnetic gears independently optimized to maximize VTD, torque per dollar (TPD), or gravimetric torque density (GTD). Additionally, this study investigates the impact of end-effects on the optimal design parameters and performance metrics. The optimal designs were determined using a genetic algorithm (GA) to independently optimize VTD, TPD, or GTD based on 2D and 3D finite element analysis (FEA) simulations. Furthermore, a multi-objective GA optimization was used to determine the Pareto optimal front for the three metrics. The results of all simulations performed in this analysis are examined to discern the performance tradeoffs, the design trends, the interactions between the optimal values of different parameters, and the impacts of end-effects. Much of this study was previously presented in [11], but this work also illustrates the Pareto optimal fronts. Furthermore, this work introduces an additional metric, leakage adjusted VTD (LA VTD), which accounts for an axial buffer to accommodate the leakage flux.

II. Design Study Methodology

This work focuses on the coaxial radial flux magnetic gear topology with surface mounted permanent magnets, which is shown in Fig. 1. In this study, the inner, low pole count cylinder serves as the high speed rotor (HSR), the outer, high pole count cylinder is stationary, and the intermediate modulator assembly serves as the low speed rotor (LSR). The number of modulators (Q_M) is related to the number of

magnetic pole pairs on the inner structure (P_{IN}) and on the outer structure (P_{OUT}) according to the expression in (1), and the resulting gear ratio, which relates the steady-state speeds of the HSR (ω_{HS}) and LSR (ω_{LS}), is given by (2). Alternatively, the modulators could be fixed and the inner and outer cylinders allowed to rotate, which would change the sign of the gear ratio and reduce its magnitude by one. This would also reduce the low speed stall torque proportionally to the reduction in gear ratio. However, this would not have a significant impact on optimization trends.

$$Q_M = P_{IN} + P_{OUT} \tag{1}$$

$$\text{Gear Ratio} = \frac{\omega_{HS}}{\omega_{LS}} = \frac{Q_M}{P_{IN}} \tag{2}$$

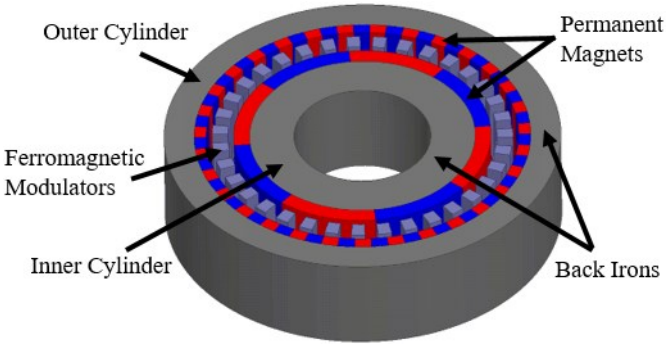

Fig. 1. Coaxial radial flux magnetic gear with surface permanent magnets

A genetic algorithm was used to independently optimize three different coaxial radial flux magnetic gear designs, one for each of the three aforementioned metrics, VTD, TPD, and GTD. Although each of the different designs was optimized to separately maximize its corresponding performance metric, every gear analyzed in the study is rated for a consistent LSR stall torque of 500 N·m with a nearest integer gear ratio of 5 and uses the same pair of active materials specified in Table I. Furthermore, the study was first conducted using 2D finite element analysis simulations, and then it was repeated to find the designs optimizing each of the three metrics based on 3D FEA simulations in order to characterize the impact of end effects. Also, a fourth metric, leakage adjusted VTD (LA VTD) was considered and independently optimized based on 3D simulations. Additionally, a multi-objective GA was used to characterize the Pareto optimal fronts for VTD, TPD, and GTD based on both 2D FEA results and 3D FEA results. In this study, VTD is defined as the LSR stall torque divided by the volume of the smallest cylinder that encloses all of the active material, as shown in (3). To calculate LA VTD, the cylinder is extended axially to the distance at which the rms magnetic flux density axially beyond the modulators is 50 mT. This is the same as adding a buffer to the stack length in (3) to accommodate this flux density on both ends of the gear. It is critical to consider the extent of the axial leakage flux because this flux can cause eddy current losses in nearby structural material, as has been the case with previous magnetic gear prototypes [2], [12]. While these losses depend on numerous factors, such as the magnetic gear pole counts, rotational speeds, and conductivity of the structural material, this analysis uses the 50 mT limit as a simple way to quantify the extent of this leakage flux. The axial leakage flux is evaluated on a circular path axially beyond the modulators, which is where it is generally the strongest [13]. TPD is the LSR stall torque divided by the active material cost (the sum of the mass of each active material multiplied by its cost rate). While the TPD value is heavily dependent on the assumed cost rates listed in Table I, the optimal design parameters and trends are relatively independent of these settings, as long as the magnet cost rate is significantly greater than that of the steel, which comprises the back irons and modulators [10]. GTD is the LSR stall torque divided by the total mass of the active materials. These calculations neglect all structural materials and only consider the permanent magnets, modulators, and back irons. Also, they ignore any manufacturing or material cost penalties associated with the quantities or dimensions of individual pieces.

$$\text{VTD} = \frac{\text{LSR Stall Torque}}{(\text{Outer Radius})^2 \cdot (\text{Stack Length})} \tag{3}$$

TABLE I. CHARACTERISTICS OF MAGNETIC GEAR ACTIVE MATERIALS

Material	Density	B_r	Cost Rate
N42 NdFeB	7400 kg/m^3	1.3 T	\$50/kg
M47 Steel (26 Gauge)	7870 kg/m^3	N/A	\$3/kg

Genetic algorithms are frequently employed for the design and optimization of electric machines [14]-[16], and this study uses the GOSET GA described in [17] to optimize the gear designs. GAs use the survival of the fittest concept to optimize design functions. The algorithm produces a generation of design cases, retains the "fittest" (highest performing) cases, produces a new generation similar to the previous generation's best cases, and then repeats the process. Each case consists of a set of specific gene values representing the parameter values of the design. Each case's VTD, TPD, or GTD determines its fitness, depending on the optimization objective. Aside from selecting values similar to the previous generation's most fit individuals (cases), the GOSET algorithm incorporates more advanced optimization techniques to introduce diversity into the population, thus ensuring that no single solution dominates the final solution too early in the optimization process. For example, it evaluates the proximity of each design case to similar cases and penalizes less diverse cases.

Table II provides the range of values considered for each design parameter. Each case is evaluated by magnetostatic 2D FEA to determine the stack length necessary to achieve the 500 N·m LSR stall torque. For the optimizations based on 3D simulations, a magnetostatic 3D FEA simulation is performed at the stack length predicted by the 2D simulation of the same cross-sectional design and, based on the result, the stack length is linearly re-scaled to achieve the 500 N·m stall torque. However, one exception to this procedure is that designs requiring stack lengths greater than 150 mm are assumed to be suboptimal and to experience only a minimal impact on torque

from end-effects; therefore, these designs were not simulated using 3D FEA models. For each case, the cross-sectional design parameters summarized in Table II and the required stack length, in conjunction with the material properties in Table I, determine the associated VTD, TPD, and GTD.

TABLE II. MAGNETIC GEAR DESIGN PARAMETERS

Name	Description	Range	Units
G_R	Approximate gear ratio	5	
P_{IN}	Inner pole pairs	3 – 30	
R_{Out}	Outer back iron outer radius	75 – 150	mm
T_{INBI}	Inner back iron thickness	5 – 25	mm
T_{INPM}	Inner magnet thickness	2.5 – 12.5	mm
T_{AG}	Air gap thicknesses	1	mm
T_{Mods}	Modulator thickness	5 – 20	mm
k_{PM}	Outer magnet thickness ratio	0.5 – 1	
T_{OUTBI}	Outer back iron thickness	5 – 25	mm
α_{INPM}	Inner magnet tangential fill factor	0.01 – 1	
α_{Mods}	Modulators tangential fill factor	0.01 – 0.99	
α_{OUTPM}	Outer magnet tangential fill factor	0.01 – 1	

Due to strong interdependencies between the effects of different dimensions, the values of certain variables are coupled through derived parameters, which are included in Table II. First, G_R, which represents the nearest integer gear ratio, was used with P_{IN} to determine the number of outer pole pairs (P_{OUT}), as shown in (4). This equation ensures that the number of modulators is even, which causes a symmetrical cancellation of the net forces on each rotor. Additionally, this approach maintains a relatively high least common multiple (LCM) between P_{IN} and P_{OUT}, which reduces the gear's torque ripple [4]. Second, k_{PM} controls the relationship between the radial thicknesses of the outer magnets (T_{OUTPM}) and the inner magnets (T_{INPM}) according to (5). This is advantageous because there is significantly greater flux leakage between adjacent poles on the outer cylinder than there is on the inner cylinder, due to the higher number of poles on the outer cylinder. Therefore, it is generally most effective to concentrate more of the permanent magnet material on the inner cylinder, especially with high gear ratios. However, if k_{PM} is too low, the inner magnets may demagnetize the outer magnets. The use of both G_R and k_{PM} was derived from [10].

$$P_{OUT} = \begin{cases} (G_R - 1)\cdot P_{IN} + 1 & \text{for } G_R \cdot P_{IN} \text{ odd} \\ (G_R - 1)\cdot P_{IN} + 2 & \text{for } G_R \cdot P_{IN} \text{ even} \end{cases} \quad (4)$$

$$T_{OUTPM} = k_{PM} \cdot T_{INPM} \quad (5)$$

III. RESULTS

During the course of the study, over 61,000 unique 2D simulations and 24,000 unique 3D simulations were run. Fig. 2(a) and Fig. 2(b) show the performances achieved by all of the evaluated designs based on 2D and 3D simulations, respectively, while Fig. 2(c) illustrates the leakage adjusted VTD results for the same 3D simulations. Fig. 2(d) illustrates the Pareto optimal fronts for maximizing all three metrics for each of the data sets shown in Figs. 2(a)-(c). Fig. 2 characterizes a significant tradeoff between VTD and TPD. In the evaluated design space, the highest VTD designs cost approximately twice as much as the highest TPD designs, while the highest TPD designs require about twice as much volume as the highest VTD designs. If the cost and weight of structural materials were considered, it would likely reduce the magnitude of this tradeoff because the larger size of the highest TPD designs would result in larger structural material costs than those of the highest VTD designs. The maximum GTD designs represent a compromise, as they achieve higher VTD values than the maximum TPD designs and higher TPD values than the maximum VTD designs. Additionally, Fig. 2 shows that the end-effects quantified by the 3D simulations have the most significant impact on the maximum VTD designs and much less impact on the maximum TPD designs. Similarly, the axial buffer for leakage flux has a greater impact on the volumes required by the maximum VTD designs than on those required by the maximum TPD designs. Both of these phenomena are strongly related to the stack lengths of the designs, as designs with larger stack lengths often experience less significant end-effects [10], [13]. Thus, the extent to which end-effects will impact the results is determined by the range of the design space relative to the target stall torque. For example, if the design space includes relatively larger outer radii, those designs will generally require shorter stack lengths to achieve the target torque and suffer a more significant reduction in torque from end-effects. Also, for a given parametric design space, lowering the target stall torque will reduce the required stack lengths, which will make the impact of end-effects more significant.

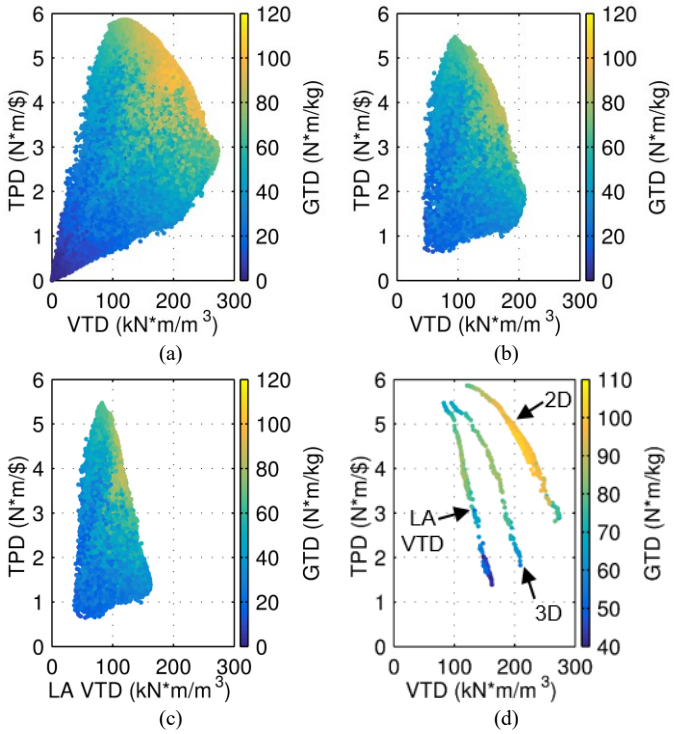

Fig. 2. Performances of designs based on (a) 2D simulations, (b) 3D simulations, and (c) 3D simulations with an axial buffer and (d) the Pareto optimal fronts maximizing VTD (or LA VTD), TPD, and GTD

Table III summarizes the design parameters and performances of the seven different optimal designs generated by the GA to independently maximize VTD or LA VTD, TPD, and GTD, based on either 2D or 3D simulations. Figs. 3(a) - 3(c) illustrate the diverging evolutions of the VTDs, TPDs, and GTDs achieved by the three different optimum designs, as denoted in Fig. 3(d), throughout the 2D simulation GA generations. These results neglect the additional size, mass, and cost of structural material. The maximum TPD designs would likely require the most structural material due to their large stack lengths and diameters. However, due to the maximum VTD designs' small volumes, any structural material would likely reduce the maximum VTDs significantly, especially when including a buffer for the axial leakage flux.

TABLE III. OPTIMAL DESIGN PARAMETERS AND PERFORMANCES

Parameter	Maximum VTD			Maximum TPD		Maximum GTD	
	2D	3D	LA	2D	3D	2D	3D
G_R	5	5	5	5	5	5	5
P_{IN}	9	7	5	17	20	13	15
R_{Out} (mm)	150	106	75	150	150	150	150
T_{INBI} (mm)	20.9	6.0	5.0	5.0	5.0	5.0	5.0
T_{INPM} (mm)	12.5	12.5	12.0	3.1	2.5	7.2	6.9
T_{AG} (mm)	1	1	1	1	1	1	1
T_{Mods} (mm)	5.6	5.3	5.0	5.0	5.1	5.0	5.0
k_{PM}	0.65	0.57	0.51	0.55	0.53	0.57	0.51
T_{OUTBI} (mm)	5.0	5.0	5.0	5.0	5.0	5.0	5.0
α_{INPM}	0.99	0.99	0.98	0.75	0.75	0.80	0.88
α_{Mods}	0.55	0.53	0.55	0.47	0.41	0.49	0.41
α_{OUTPM}	0.98	0.97	0.99	0.84	0.85	0.90	1.0
Stack Length (mm)	25.9	67.6	146.9	58.5	74.2	33.9	40.6
Axial Buffer (mm)	N/A	14.4	13.6	N/A	5.7	N/A	9.7
VTD (kN·m/m^3)	274	210	193	121	95	209	174
LA VTD (kN·m/m^3)	N/A	147	162	N/A	83	N/A	118
TPD (N·m/$)	2.89	1.83	1.39	5.86	5.47	4.57	3.76
GTD (N·m/kg)	66.5	54.2	40.8	78.3	65.5	102.8	86.8

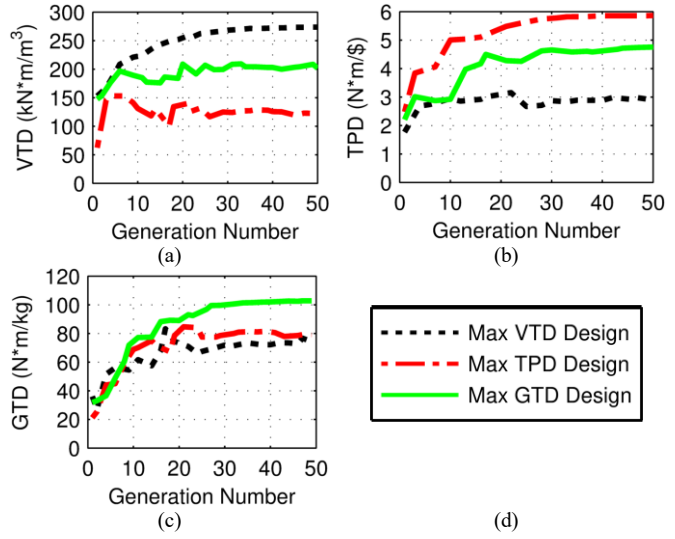

Fig. 3. GA driven evolution of the (a) VTD, (b) TPD, and (c) GTD of (d) the three optimal designs based on 2D simulations

Fig. 4 shows the variations in the optimal design performances as the outer radius varies. Based on 2D FEA, increasing the outer radius improves all three metrics, but the percentage improvement of the VTD is less than that of the TPD and GTD. Increasing the outer radius linearly raises the air gap area and the torque arm, which quadratically improves a design's 2D stall torque. However, it also quadratically increases the cross-sectional area, so the VTD increases sub-linearly with outer radius [18]. Alternatively, the magnet and steel cross-sectional areas only increase linearly with the radius, so the TPD and GTD increase linearly with the outer radius. End-effects further complicate these trends because increasing the radius decreases the stack length (for a fixed torque), which increases the impact of axial leakage flux and reduces the advantages gained by increasing the radius. This decreases the optimal outer radius for VTD and LA VTD, but not for TPD and GTD (in this study). Additionally, for a given outer radius the maximum TPD and GTD designs have longer stack lengths than the maximum VTD design, so they suffer less from end-effects at that radius. This also resulted in the optimal TPD designs for small outer radii not being simulated in 3D, due to the 150 mm stack length constraint.

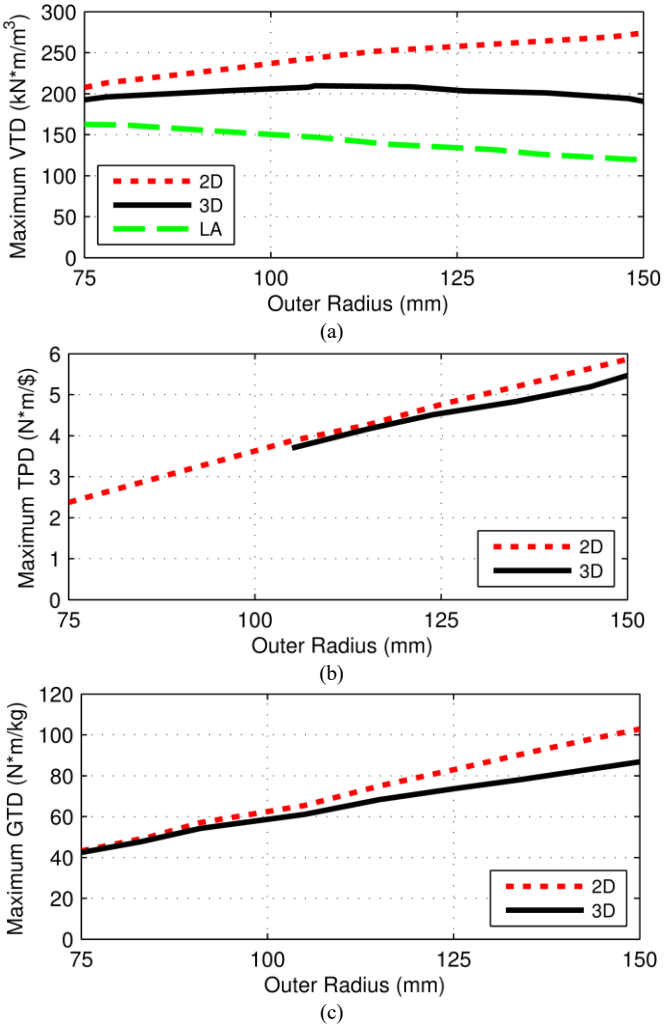

Fig. 4. Variation of (a) maximum VTD, (b) maximum TPD, and (c) maximum GTD with outer radius

Fig. 5 shows the envelopes illustrating the optimal performances achieved as the inner magnet thickness varies. Magnet volume is a major aspect of the tradeoff between VTD and TPD, and magnet thickness is one of the dominant factors in determining the magnet volume. Accordingly, Fig. 5 illustrates significantly different trends for optimizing VTD, TPD, and GTD. Because increasing the magnet thickness increases the effective air gap, the torque returns diminish as magnet thickness continues to increase. Therefore, while high VTD designs generally have very thick magnets, high TPD designs often have much thinner magnets to make more cost-effective use of the expensive magnet material. Optimal GTD designs usually have intermediate magnet thicknesses. At some optimal thickness, the additional torque produced by increasing the magnet thickness does not outweigh the added mass of the magnets. Additionally, Fig. 5 indicates that increasing magnet thickness tends to increase the impact of end-effects. This occurs because increasing the magnet thickness generally reduces the stack length required to achieve the target torque. Thus, when end-effects are considered, the torque returns gained by increasing the magnet thickness diminish even faster.

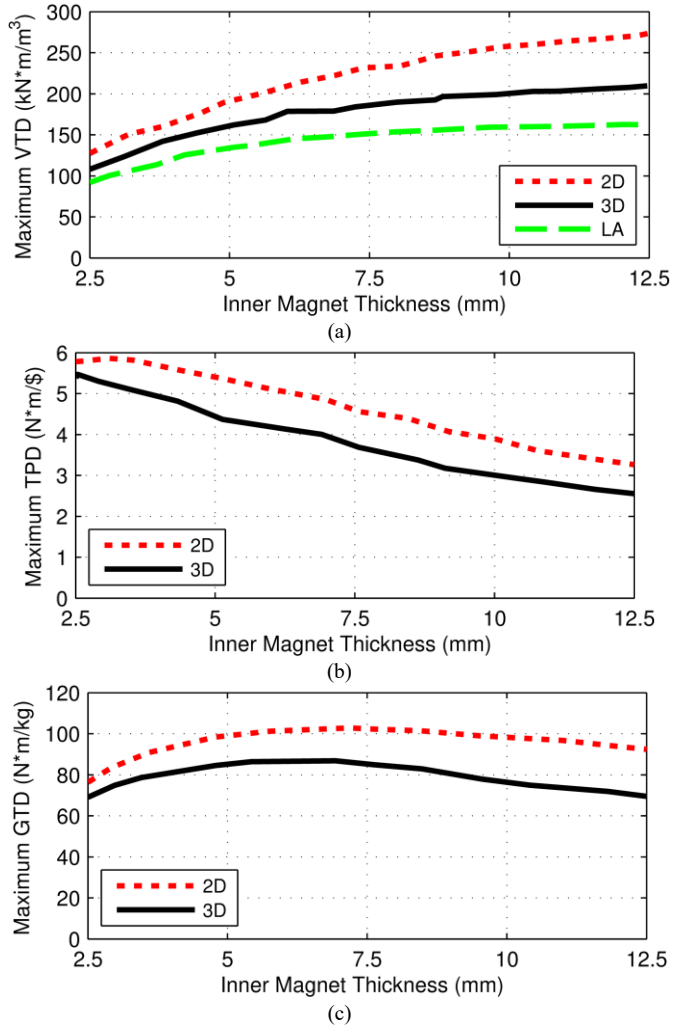

Fig. 5. Variation of (a) maximum VTD, (b) maximum TPD, and (c) maximum GTD with inner magnet thickness

Fig. 6 shows the envelopes illustrating the optimal performances achieved as the inner pole pair count varies. There are a few different factors that affect the optimal pole count. First, the magnet thicknesses impact the effective air gap, which significantly influences the optimal pole arc. Larger effective air gaps result in increased leakage flux between adjacent poles, which tends to favor larger optimal pole arcs. Larger pole arcs are achieved by reducing the pole pair count. Thus, the thicker magnets in the optimal VTD designs usually favor lower pole pair counts than the thinner magnets in the optimal TPD designs. Because the magnets in the optimal GTD designs have intermediate thicknesses, the optimal GTD designs have optimal pole pair counts between those of the optimal VTD and optimal TPD designs. Conversely, selecting a fixed pole pair count affects the performance trends as magnet thickness is varied. The pole arcs are also affected by the air gap radii, which are determined by the different radial thickness parameters and the outer radius. Therefore, because the outer radii of the optimal 3D VTD design and the optimal LA VTD design are lower than that of the optimal 2D VTD design, the optimal 3D VTD and LA VTD designs favor lower pole pair counts.

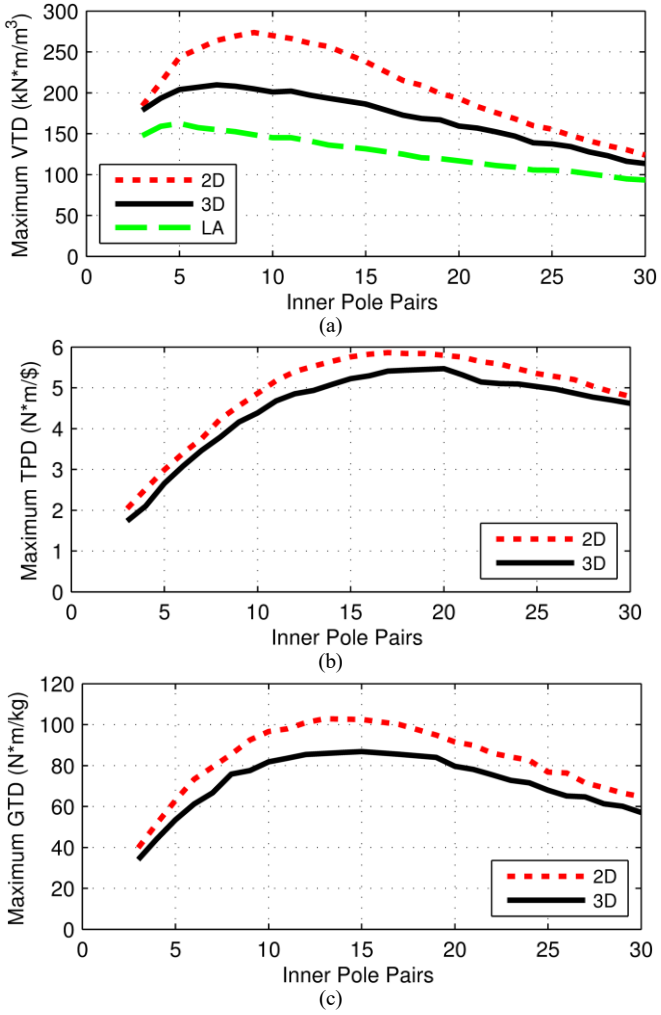

Fig. 6. Variation of (a) maximum VTD, (b) maximum TPD, and (c) maximum GTD with inner pole pair count

Fig. 7 shows the envelopes of the optimal performances achieved as the back iron thicknesses vary. Increasing the thickness of the outer back iron significantly decreases the torque because it reduces the air gap radii, which are where the torque is produced. Thus, all three metrics favor designs with very thin outer back irons. While saturation of the outer back iron can reduce the torque, the impact of iron saturation is relatively small compared to the large linear reluctances of the two air gaps and two sets of permanent magnets. Generally, mechanical considerations, rather than excessive iron saturation, will determine the minimum outer back iron thickness. On the other hand, the thickness of the inner back iron has a very small impact on torque because it does not affect the air gap radii (based on the independent design parameters used in this study). However, the inner back iron thickness impacts the material cost and mass of the gear, so the optimal TPD and GTD designs favor very thin inner back irons. Another major consideration for sizing the back irons is magnetic flux containment. If the back irons are too thin, magnetic flux will leak beyond them, which could cause eddy current losses in structural material or create a hazard. However, this study neglects the issue of flux containment.

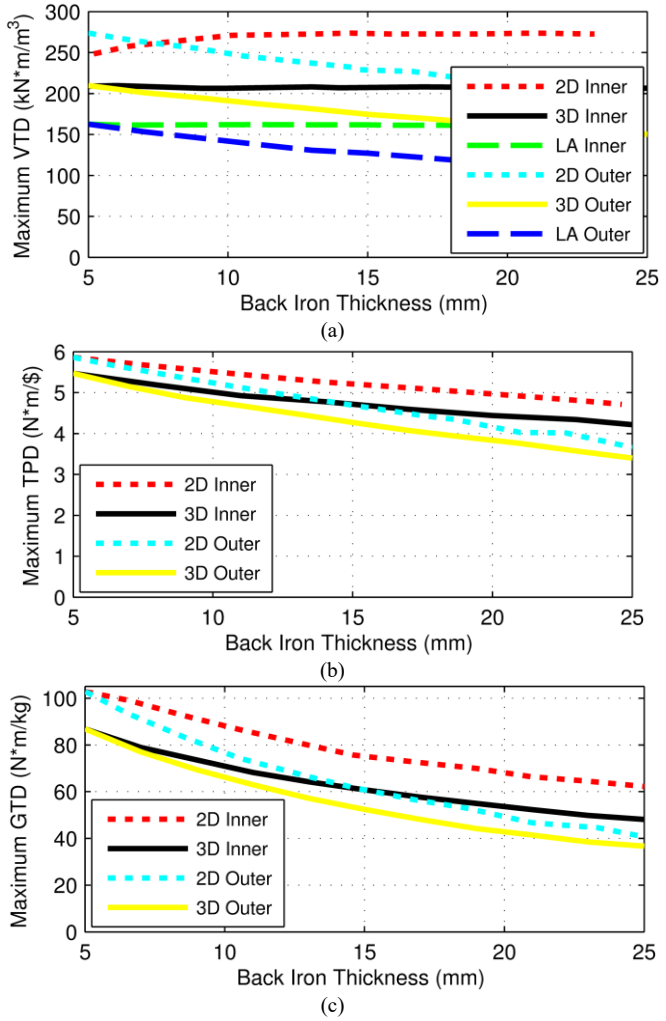

Fig. 7. Variation of (a) maximum VTD, (b) maximum TPD, and (c) maximum GTD with inner and outer back iron thicknesses

Fig. 8 shows the envelopes of the optimal performances as the modulator fill factor varies. While a modulator fill factor slightly greater than 0.5 can provide the most torque for the optimal VTD designs, increasing the fill factor adds material cost and mass to the design. Additionally, the optimal pole pair count affects the optimal modulator fill factor. With a higher pole pair count, the modulators and the slots between adjacent modulators become tangentially narrower, which results in increased flux leakage between adjacent modulators. However, this increased flux leakage can be counteracted by slightly lowering the modulator fill factor. Accordingly, the optimal TPD and optimal GTD designs favor fill factors slightly below 0.5. Another interesting finding is that the 3D simulations tend to favor slightly lower modulator fill factors than the 2D simulations. This occurs in part because a significant portion of the axial flux at the ends of the magnetic gear passes through the modulators [13]. Therefore, smaller modulators increase the reluctance "seen" by axially escaping leakage flux and generally reduce the impact of end-effects on the magnetic gear torque rating. Ultimately, in most cases, a modulator fill factor of 0.5 is fairly close to optimal for all three metrics.

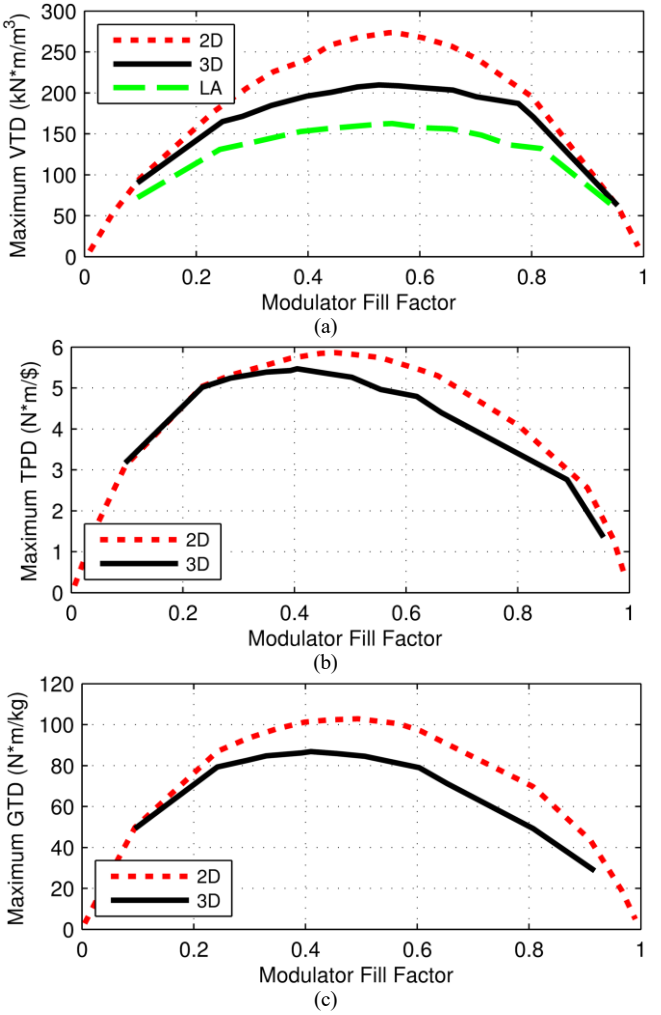

Fig. 8. Variation of (a) maximum VTD, (b) maximum TPD, and (c) maximum GTD with modulator fill factor

Fig. 9 shows the envelopes of the optimal performances as the magnet fill factors vary. Generally, increasing either of the magnet fill factors results in increased torque due to an increase in the magnitude of the fundamental spatial harmonic of the magnetomotive force (MMF) from that set of magnets. However, the torque returns diminish as the magnet fill factors continue to increase towards 1. Additionally, increasing the magnet fill factors increases the magnet volume, which significantly increases the material cost of the magnetic gear; therefore, the optimal TPD designs favor lower magnet fill factors than those required for the optimal VTD designs. Furthermore, because increasing the magnet fill factors tends to reduce the stack length required to achieve the target stall torque, the designs with higher magnet fill factors also generally experience more significant end-effects. Nonetheless, all three metrics converge to optimal designs with relatively high magnet fill factors of at least 0.75 on both the inner and outer cylinders. This study considered ideal arc shaped magnets; however, in addition to creating a non-uniform air gap, using rectangular magnets would also place practical limits on the maximum achievable magnet fill factors.

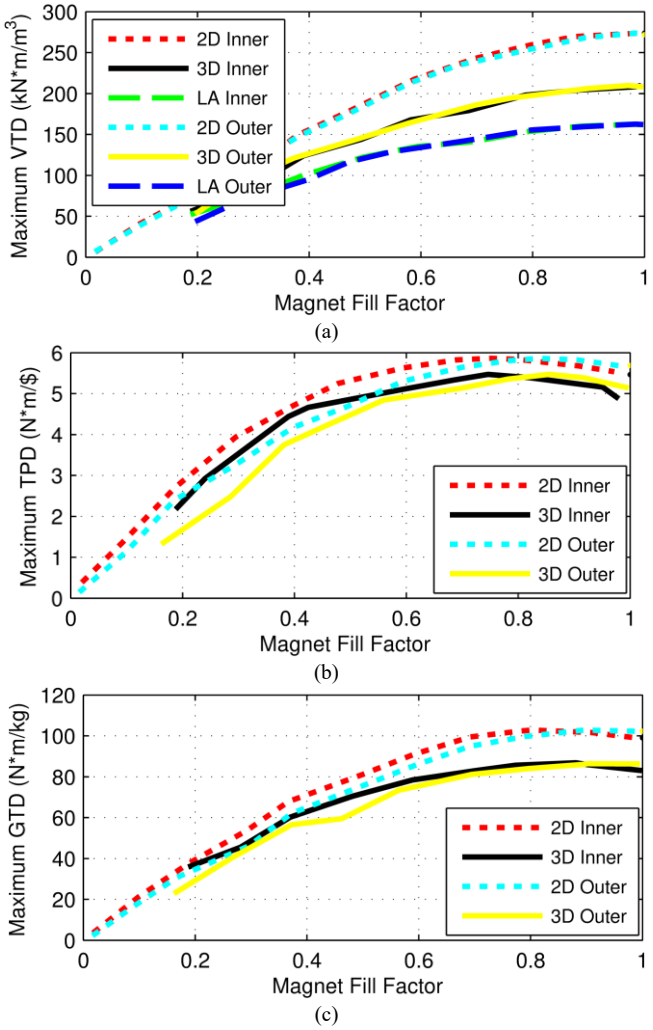

Fig. 9. Variation of (a) maximum VTD, (b) maximum TPD, and (c) maximum GTD with magnet fill factors

Fig. 10 shows the envelopes of the optimal performances as the modulator thickness varies. Increasing the modulator thickness reduces the inner air gap radius for a given outer radius, so it generally reduces a gear's stall torque. Additionally, increasing the modulator thickness increases the leakage flux both in the modulators and in the slots between adjacent modulators, which can further decrease the torque. Therefore, the optimal designs for each of the three metrics have relatively thin modulators. Nonetheless, the modulator layer must be thick enough that the reluctance of the slots between adjacent modulators is large enough that the flux is modulated by the alternating reluctances of the modulators and the slots. However, in most cases, mechanical concerns will dictate that the modulators must be appreciably thicker than the magnetically optimal value [19]. In particular, the modulators must be thick enough to mechanically withstand the significant attractive forces from the inner and outer magnets and to transfer the torque to the LSR shaft. Additionally, the forces on individual modulators change as the gear operates, and the modulators should be stiff enough to minimize vibrations from these varying forces.

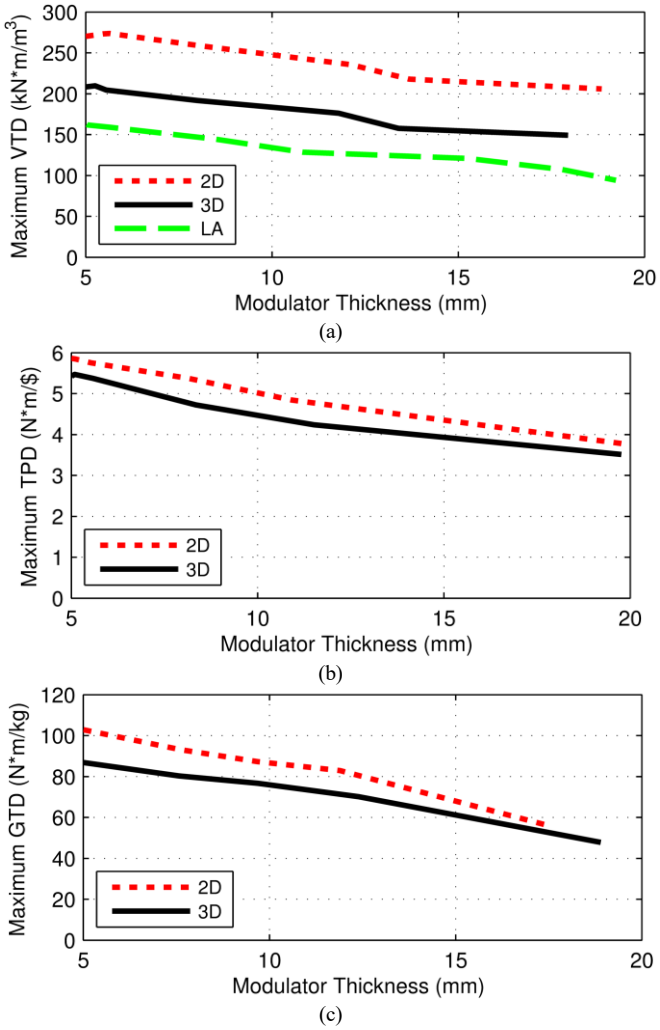

Fig. 10. Variation of (a) maximum VTD, (b) maximum TPD, and (c) maximum GTD with modulator thickness

Fig. 11 shows the envelopes of the optimal performances as the magnet thickness ratio varies. While increasing the magnet thickness ratio increases the amount of magnet present in the gear, it also reduces the air gap radii (for a fixed outer radius). Additionally, because the outer magnets have a much higher pole count, there is significantly more leakage flux between adjacent poles when the outer magnet thickness is increased. Accordingly, increasing the magnet thickness ratio does not have a large overall impact on the VTD of the design. However, because adding magnet material on the outer cylinder increases the cost and mass of the magnetic gear, the optimal TPD and GTD designs converge to lower optimal magnet thickness ratios. The minimum outer magnet thickness may often be limited by manufacturing considerations, such as the minimum practical magnet thickness. Additionally, if the magnet thickness ratio is too low, the flux from the inner magnets may demagnetize the outer magnets, especially if the gear is operated at high temperatures. While this analysis only considers a single gear ratio, a past study [10] shows that the gear ratio affects the extent of these magnet thickness ratio design trends.

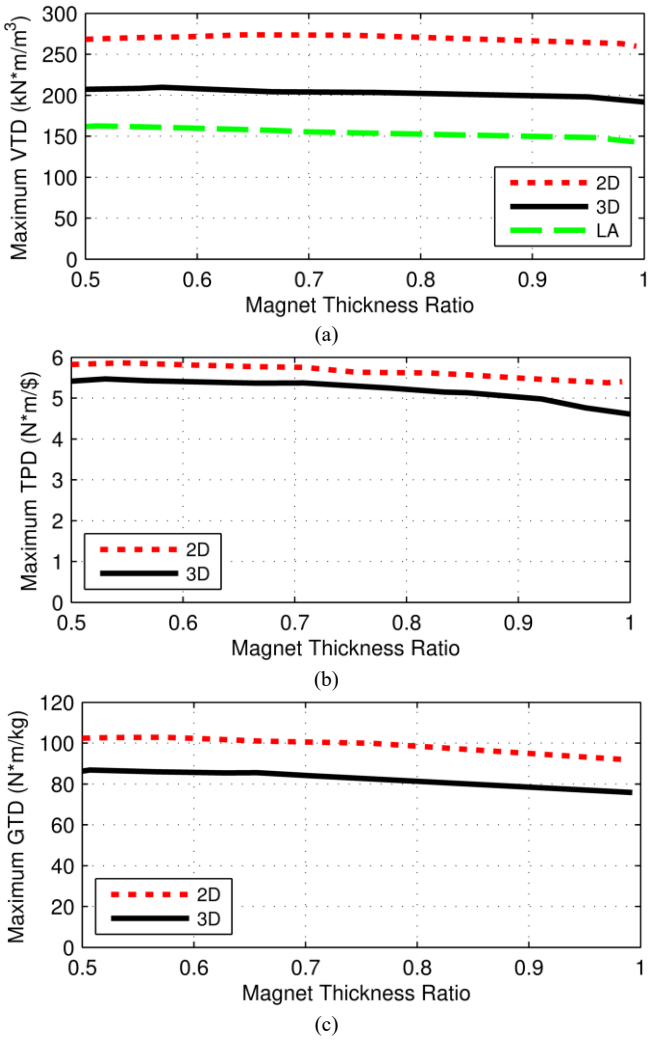

Fig. 11. Variation of (a) maximum VTD, (b) maximum TPD, and (c) maximum GTD with magnet thickness ratio

IV. Conclusions

A genetic algorithm was used to independently optimize different coaxial radial flux magnetic gear designs for maximum volumetric torque density (VTD), maximum torque per dollar (TPD), and maximum gravimetric torque density (GTD) based on both 2D simulations and 3D simulations within a parametric design space. The maximum VTD obtained was 274 kN·m/m^3 based on 2D simulations and 210 kN·m/m^3 based on 3D simulations; the maximum leakage adjusted VTD obtained was 162 kN·m/m^3. The maximum TPD obtained was 5.86 N·m/$ based on 2D simulations and 5.47 N·m/$ based on 3D simulations. The maximum GTD obtained was 102.8 N·m/kg based on 2D simulations and 86.8 N·m/kg based on 3D simulations. The difference between 2D and 3D results is dependent on the magnetic gear's form factor, which is determined by the design space (especially the maximum permissible outer radius) and the target torque. Larger torques require longer stack lengths, which reduce the relative impact of end-effects. In this study, the design space and required torque favored form factors characterized by relatively short stack lengths and relatively wide diameters. This led to significant end-effects, especially for the optimal VTD designs.

There are stark differences between the optimal VTD, TPD, and GTD designs. The optimal VTD designs favor significantly thicker magnets and higher magnet volumes than the optimal TPD designs. The difference in optimal magnet thicknesses also results in a difference in the optimal pole pair counts required for the optimal VTD and optimal TPD designs. The optimal GTD designs tend to have optimal parameter values between those of the maximum VTD and maximum TPD designs. These differences resulted in the VTDs of the maximum TPD designs being much lower than those of the maximum VTD designs and the TPDs of the maximum VTD designs being much lower than those of the maximum TPD designs. However, the maximum GTD designs achieved a good compromise in performance between VTD and TPD. Nonetheless, all of the optimal designs have very thin outer back irons, modulators that are very radially thin, and modulator fill factors near 0.5.

Considering end-effects significantly impacted both optimal design performance predictions and optimal parameter value selections. Many designs experienced a significant reduction in torque transmission capabilities, which necessitated a corresponding increase in stack length to maintain the target torque rating. Furthermore, because several design parameters influence the significance of end-effects, the optimal design parameters also changed once this important phenomenon was considered in the analysis. Notably, considering 3D effects significantly reduced the optimal outer radius for the maximum VTD designs. This resulted in a reduction in the optimal pole pair count. If the VTD is adjusted to provide an axial buffer for the leakage flux so that it does not cause losses in nearby conductive materials, the optimal radius and optimal pole pair count are reduced even further. Additionally, consideration of end-effects slightly decreased the optimal modulator fill factor required to maximize each metric. These results clearly demonstrate that 3D end-effects can dramatically reduce the torque ratings of

certain magnetic gear designs, and they should be considered in studies of magnetic gears with relatively short stack lengths and wide diameters in order to ensure the correct selection of proper optimal design parameters.

ACKNOWLEDGMENT

The authors would like to thank ANSYS for its generous support of the EMPE lab through the provision of FEA software.

REFERENCES

[1] K. Atallah and D. Howe, "A novel high-performance magnetic gear," *IEEE Trans. Magn.*, vol. 37, no. 4, pp. 2844–2846, Jul. 2001.

[2] P. O. Rasmussen, T. O. Anderson, F. T. Jorgensen, and O. Nielsen, "Development of a High Performance Magnetic Gear," *IEEE Trans. Ind. Appl.*, vol. 41, no. 3, pp. 764-770, May/June 2005.

[3] P. M. Tlali, R.-J. Wang, and S. Gerber, "Magnetic gear technologies: A review," in *Proc. Int. Conf. Elect. Mach.*, 2014, pp. 544–550.

[4] N. W. Frank and H. A. Toliyat, "Gearing ratios of a magnetic gear for wind turbines," in *Proc. IEEE Int. Elect. Mach. Drives Conf.*, 2009, pp. 1224–1230.

[5] K. K. Uppalapati, J. Z. Bird, D. Jia, J. Garner, and A. Zhou, "Performance of a magnetic gear using ferrite magnets for low speed ocean power generation," in *Proc. IEEE Energy Convers. Congr. Expo.*, 2012, pp. 3348–3355.

[6] L. MacNeil, B. Claus, and R. Bachmayer, "Design and evaluation of a magnetically-geared underwater propulsion system for autonomous underwater and surface craft," in *Proc. Int. Conf. IEEE Oceans*, 2014, pp. 1-8.

[7] T. V. Frandsen, L. Mathe, N. I. Berg, R. K. Holm, T. N. Matzen, P. O. Rasmussen, and K. K. Jensen, "Motor integrated permanent magnet gear in a battery electrical vehicle," *IEEE Trans. Ind. Appl.*, vol. 51, no. 2, pp. 1516–1525, Mar./Apr. 2015.

[8] K. K. Uppalapati, J. Z. Bird, J. Wright, J. Pitchard, M. Calvin, and W. Williams, "A magnetic gearbox with an active region torque density of 239Nm/L," in *Proc. IEEE Energy Convers. Congr. Expo.*, 2014, pp. 1422-1428.

[9] M. Johnson, M. C. Gardner, and H. A. Toliyat, "Analysis of axial field magnetic gears with Halbach arrays," in *Proc. IEEE Int. Elect. Mach. Drives Conf.*, 2015, pp 108-114.

[10] M. Johnson, M. C. Gardner, and H. A. Toliyat, "Design Comparison of NdFeB and Ferrite Radial Flux Magnetic Gears," in *Proc. IEEE Energy Convers. Congr. Expo.*, 2016, pp 1-8.

[11] M. C. Gardner, B. E. Jack, M. Johnson, and H. A. Toliyat, "Comparison of Coaxial Radial Flux Magnetic Gears Independently Optimized for Volume, Cost, and Mass," in *Proc. IEEE Int. Elect. Mach. Drives Conf.*, 2017, pp 1-8.

[12] S. Gerber and R. J. Wang, "Evaluation of a prototype magnetic gear," in *Proc. IEEE Int. Conf. Ind. Technol.*, 2013, pp. 319-324.

[13] S. Gerber and R-J. Wang, "Analysis of the end-effects in magnetic gears and magnetically geared machines," in *Proc. IEEE Int. Conf. Elect. Mach.*, 2014, pp. 396-402.

[14] T. D. Nguyen, V. Lanfranchi, C. Doc and J. P. Vilain, "Comparison of optimization algorithms for the design of a brushless DC machine with travel-time minimization," in *Proc. ELECTROMOTION,* 2009, pp. 1-6.

[15] S. Stipetic, W. Miebach and D. Zarko, "Optimization in design of electric machines: Methodology and workflow," in *Proc. ACEMP – OPTIM – ELECTROMOTION*, 2015, pp. 441-448.

[16] A. Krishnamoorthy and K. Dharmalingam, "Application of Genetic Algorithms in the Design Optimization of Three Phase Induction Motor", *J. Comput. Applicat.*, vol. 2, no. 4, pp. 1 – 5, Oct – Dec. 2009.

[17] S. D. Sudhoff and Y. Lee, "Energy systems analysis consortium (ESAC) genetic optimization system engineering tool (GOSET) version manual," School Electr. Comput. Eng., Purdue Univ., West Lafayette, IN, 2003.

[18] M. Johnson, M. C. Gardner, and H. A. Toliyat, "Design and Analysis of an Axial Flux Magnetically Geared Generator," *IEEE Trans. Ind. Appl.*, vol. 53, no. 1, pp. 97-105, Jan./Feb. 2017.

[19] D. J. Evans and Z. Q. Zhu, "Influence of design parameters on magnetic gear's torque capability," in *Proc. IEEE Int. Elect. Mach. Drives Conf.*, 2011, pp. 1403-1408.